JOURNAL OF PROPULSION AND POWER
Vol. 18, No. 1, January–February 2002

Overview of the Development of Hydrazinium Nitroformate

H. F. R. Schöyer*
Schöyer Consultancy B.V., 2726 DV Zoetermeer, The Netherlands
W. H. M. Welland-Veltmans†
Aerospace Propulsion Products, 4791 RT Klundert, The Netherlands
J. Louwers‡
Royal Philips Electronics, Optical Storage, 5600 JB Eindhoven, The Netherlands
and
P. A. O. G. Korting,§ A. E. D. M. van der Heijden,¶ H. L. J. Keizers,** and R. P. van den Berg**
TNO-Prins Maurits Laboratorium, 2280 AG Rijswijk, The Netherlands

Hydrazinium nitroformate (HNF) has been under renewed development since the late 1980s. These research and development efforts have demonstrated that it is possible to produce HNF crystals with acceptable morphology and stability. Although the production of HNF is based on a simple acid–base reaction, the resulting product strongly depends on the synthesis and crystallization techniques used. For a propellant oxidizer, control of size (distribution) in the production phase of the crystals is important. The effect of different crystallization processes has been investigated, and the results are reported. Stability depends, among other factors, on purity and/or contamination. A promising method to determine the hydrazine and nitroform content of HNF is being discussed. Because it is demonstrated that excess hydrazine in HNF strongly affects HNF stability, such a method is important for quality control. Sonocrystallization allows improving the HNF morphology. In addition, sonocrystallization also led to improved thermal stability of the oxidizer. Cocrystallization permits the inclusion of ballistic modifiers or stabilizers in the crystals or the application of coatings during the crystallization process. This process may also increase the tap density. The slow natural decomposition of HNF during storage is demonstrated to be a first-order reaction; it permits calculating that, at room temperature, HNF may be safely stored for hundreds of years. The primary HNF decomposition products and the most likely initial decomposition/combustion mechanism have been identified, which helps in understanding the overall decomposition process. The surface temperature of burning HNF has been measured; it is strongly dependent on the pressure at which the combustion takes place. Finally, it was demonstrated that several ingredients affect the burning rate exponent of neat HNF.

Nomenclature

A	=	rate constant
C	=	constant
D	=	diameter
E	=	activation energy
G	=	gas production in vacuum thermal stability
L	=	length
n	=	burning rate exponent in $r = a \cdot p^n$
pH	=	$-^{10}\log(H_3O^+)$
R	=	universal gas constant
r	=	reaction rate
T	=	temperature
t	=	time
x	=	characteristic particle size
ρ	=	density

Subscripts/Superscripts/Indices

b	=	binder
m	=	melting
p	=	at constant pressure
sp	=	specific
T	=	temperature
tap	=	tap
50	=	for which 50% of the total distribution is smaller

I. Introduction

DURING the last half-decade, the development of hydrazinium nitroformate (HNF) as an oxidizer for rocket propellants has progressed substantially. New methods to improve the thermal stability and to control the crystal size were identified and have been implemented in the production process. Work was done on (co)crystallizing HNF with other ingredients such as stabilizers, and the compatibility and decomposition of HNF were investigated. The overall characteristics of HNF were investigated, the HNF morphology was improved, among other factors, by using ultrasound crystallization, and production costs were reduced. The latter was achieved by reusing washing liquids and using other ingredients, such as hydrazine hydrate. The combustion and decomposition of HNF were studied in detail, investigated experimentally, and compared with theoretical models. It became clear that the combustion of HNF essentially is different from the very slow natural decomposition that is a first-order reaction, whereas the combustion reaction is roughly between one and one-half and second order. The compatibility of HNF with a large number of materials was investigated. All of this work is summarized in this paper. Because identical methodologies were not followed in all participating laboratories and industries, it is not always possible to provide the same type of data. Some data are overlapping; most data from the various sources are complementary.

Received 23 July 2000; revision received 16 May 2001; accepted for publication 14 August 2001.

*Director, van Vrieslandhove 6. Associate Fellow AIAA.
†Chemical Engineer, P.O. Westelijke Randweg 25. Member AIAA.
‡System Architect, Emerging Technologies and Systems, P.O. Box 80002. Member AIAA.
§Director, P.O. Box 45, 2280 AA Rijswijk, The Netherlands.
¶Research Scientist, Propellant Development and Crystallization of Energetic Materials, P.O. Box 45.
**Research Scientist, Propellant Development and Engineering, P.O. Box 45.

It is concluded that much progress has been made over the past five years. The quality of HNF has improved substantially, like its morphology. The steady-state combustion of HNF is well understood by now, and experiments and combustion models agree very well.

II. HNF Production

A. Facility

The production facility, built in 1993, allows for the simple acid–base reaction that constitutes the fundamental step in the HNF manufacturing. Reactions take place in a large stirred and temperature-controlled reactor vessel. It allows for the production of 3–5 kg HNF per batch. The pilot plant has a maximum capacity of ~300-kg HNF per year. All commercially available European HNF is produced in this facility.

B. Production Methods

The manufacturing of HNF is, in principle, straightforward. The basic steps are given in Fig. 1. Water is extracted from the H_2O/nitroform (NF) mixture (which is a basic ingredient) by the addition of salt. Dichloroethane (DCE) is added to the pure NF. Hydrazine (HZ) is added under controlled conditions to the NF/DCE mixture and HNF precipitates. The remainder of the production process is to improve the quality and purity of the HNF. The different recrystallization processes, cooling crystallization (C), the solvent/nonsolvent process (S), and evaporative crystallization (E) lead to crystals with somewhat different characteristics, including size and aspect ratio (L/D), but also different stability characteristics in vacuum thermal stability (VTS) tests. The HNF that is produced after the addition of HZ to the NF/DCE mixture (HNF–P) shall meet certain requirements. In the past, a recrystallization step was necessary to improve purity, thermal stability, and morphology. Because of an improved understanding of the crystallization process, presently recrystallization is merely performed to improve morphology (L/D, x_{50}) using the S and C processes. During the E process, HNF is dissolved in isopropyl alcohol (IPA). This solution is subsequently heated, and IPA is vaporized under vacuum while HNF crystallizes. This leads to a better HNF purity, but to a noncontrolled morphology and mean crystal size.

During the S process, an HNF solution in methanol (MeOH) is added to a nonsolvent, methylene chloride (MC). The MeOH dissolves in the MC causing the HNF to precipitate. This results in small HNF crystals. Size and L/D can be controlled during this process.

During the C process, a solution of HNF in MeOH is cooled below the saturation point. Seed crystals may be used to induce the nucleation process. By controlling the cooling history, the L/D may be controlled.

Some typical production parameters used for verification and production acceptance of the HNF are the melting point T_m, the VTS values, and the pH. The morphology is determined by mean particle size, L/D, and tap density. Typical values for the four types of HNF are given in Table 1.

In most of the VTS tests it is observed that during the first $1\frac{1}{2}$ h (or less) the major gas evolution takes place; during the remainder

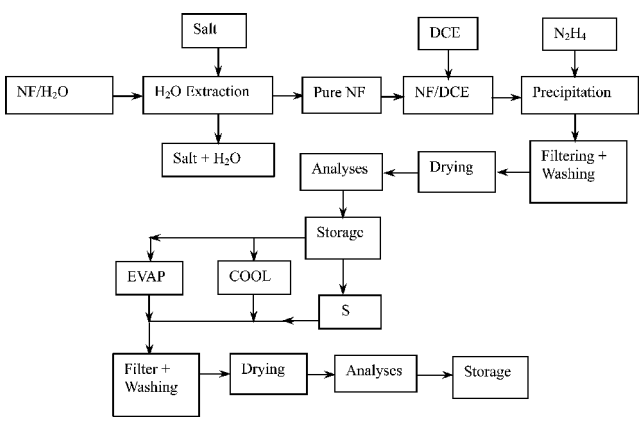

Fig. 1 Simplified schematic of the HNF production process.

Table 1 Typical values used for verification and production acceptance of HNF

Property	HNF-P	HNF-E	HNF-C	HNF-S
T_m,[a] °C	>115	>115	>116	>115
VTS (48 h, 60°C), ml/g	<0.5	<0.2	<0.5	<1.8
pH	3.8–4.2	4.3–5	4.1–4.9	4.3–4.8
D_{mean}, μm	300	500	200–1000	60–140
Typical particle range, μm	100–1500	40–1500	200–2000	50–300
L/D	1–4	3–15	<8	<8
ρ_{tap}, kg/m^3	——	——	800–1000	400–600
Appearance	Yellow rods	Yellow needle crystals	Yellow facetted dry rods	Diamond-shaped rods

[a]This is not the physical value of the melting point, but one determined by a blackbody radiometer; it gives a systematic difference with the melting point measured by oil bath submersion of 3–8°C. For production control purposes, this is acceptable.

of the 48 h, usually the amount of gas increases by not more than twice the initial gas evolution. This is an indication that much of the gas is due to the evaporation of processing and washing liquids that adhere to the surface of the HNF crystals. By the introduction of more washing and drying cycles, the VTS decreased dramatically: For example, one wash/drying cycle led to an initial VTS (60°C, $1\frac{1}{2}$ h) of ~0.54 ml/g, which, after 48 h, had increased to 0.94 ml/g; three washing and drying steps improved these values to ~0.18 ml/g and 0.36 ml/g, respectively. The melting point of the HNF was hardly affected, confirming that a substantial part of the VTS values is due to the evaporation of washing and processing fluids. Normally, intensive washing and drying cycles are not necessary.

1. *Improvement in Production Methods*

With regard to quality, cost reduction, and environmental aspects, numerous improvements have been made in the HNF production process. The major ones are discussed hereafter.

a. HNF quality control. It was not (yet) possible to determine, in one single measurement, the HZ and NF content of HNF. Usually, two separate titrimetric analyses are performed to determine separately the NF and HZ content of HNF. The determination of the amount of NF is an acid titration not specific for NF, and there is always a discrepancy between the HNF purity as determined on the basis of HZ content and NF content. Therefore, other methods have been investigated that might be used for HNF quality control during the production process. This limits the methods to those that do not require much time, manpower, or large investments. Impurities, due to processing liquids, for example, MeOH, DCE, and IPA present in HNF can easily be detected with nuclear magnetic resonance (NMR) or gas chromatography and mass spectroscopy. Impurities that are similar to HZ, for example, $N_2H_6^{2+}$, or NF, for example, dinitromethane, cannot be detected by these techniques. Other techniques such as high-performance liquid chromatography, Fourier transform infrared spectroscopy (FTIR), solid-state NMR, x-ray diffraction, and capillary electrophoresis are even more limited in their possibilities. However, an interesting technique may be the ultraviolet visual (UV-vis) spectroscopy.

Hydrazine has an ultraviolet (UV) absorption peak around 210 nm; NF has two UV absorption peaks: one around 220 nm and one at 350 nm. HNF has two absorption peaks in the UV: one around 210 nm and one at 350 nm. This is illustrated in Fig. 2. It turns out that the peak height around 210 nm is roughly the sum of the HZ peak height and NF peak height. This leads to an interesting observation: For three different concentrations of HNF in water, the heights of the 210- and 350-nm peaks may be compared, and, as Fig. 3 shows, the slope of the 210-nm peak height is twice the slope of the 350-nm peak height. In this way, it may become possible to determine the HZ/NF ratio in HNF directly, where the measurement is not affected by the presence of other acidic material. The method still needs further evaluation, but looks very promising. Because very low concentrations of HNF are being used (down to 10^{-5} mol/l) it is doubtful whether impurities can be detected by the

Table 2 Effect of using HZH instead of PAH for the production of HNF

Parameter	Typical values	Batch 1	2	3	4	5	6
HZ used	PAH	PAH	80% HZH	100% HZH	100% HZH	100% HZH	100% HZH
T_m, °C	>111	115.2	116.2	116.2	116.0	116.8	115.9
pH	3.8–5.3	4.11	3.88	3.96	4.00	3.95	4.16
VTS (60°C, 48 h), ml/g	<2.5	1.0	0.34	0.34	0.28	0.29	0.41
VTS (80°C, 100 h), ml/g		20[a]	2.8	3.8	6.0	2.4	5.2
Overall yield, %		54.1	50.1	48.0	58.8	64.0	62.9

[a] Stopped after 75 h because 20 ml/g had already evolved.

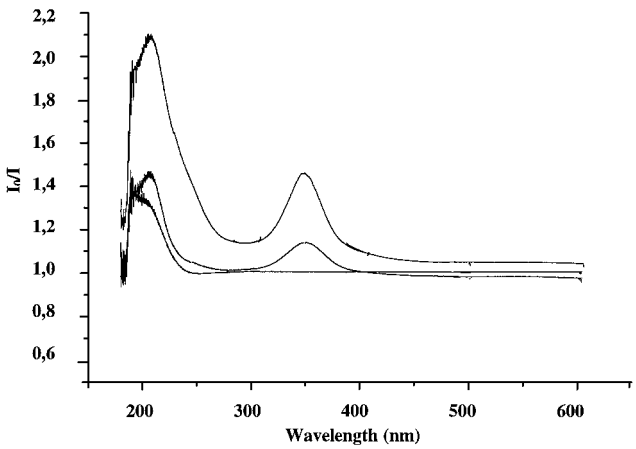

Fig. 2 UV-absorption spectra for HZ (bottom), NF (middle), and HNF (top).

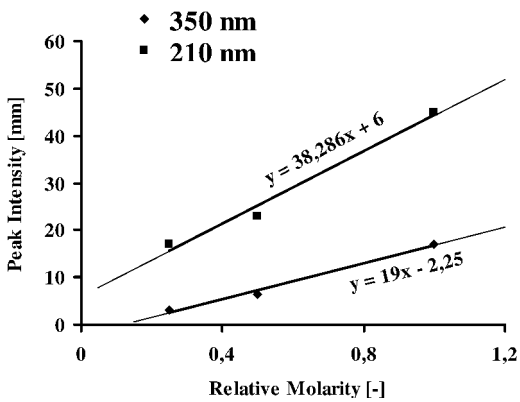

Fig. 3 Slope of the intensity of the two HNF–UV peaks.

UV-vis technique, even if these impurities would yield an absorption spectrum in the 200–600 nm range. If successful, the method will substantially reduce the cost of production control.

b. Use of hydrazine hydrate. Because it is known that HNF is sensitive to contamination, the production of HNF used purified anhydrous hydrazine (PAH) as one of its ingredients. PAH, which has a purity better than 99.25%, is rather expensive: ~€180/kg. Experiments (see Table 2) showed that using hydrazine hydrate ($N_2H_4 \cdot H_2O$) also led to good quality HNF. The costs of hydrazine hydrate (HZH) are only € 6/kg. Therefore, substantial cost savings are possible in the ingredients, whereas an additional advantage is the reduced hazard level when working with HZH instead of HZ: The heat per unit volume developed during the HZH–NF reaction is substantially lower than for the PAH–NF reaction.

Comparing the data of Table 2 shows that the VTS values for HZH-based HNF are far superior to PAH-based HNF (especially at 80°C) and that the melting temperatures have also improved while the pH is in the correct range. From a safety and quality point of view, using HZH instead of PAH for the production of HNF clearly is advantageous.

c. Reducing excess amounts of HZ or HZH. HNF and HZ are incompatible, whereas large concentrations of HNF can dissolve in HZH. It is, therefore, important that during the production of HNF, the HZ excess is limited to as low a value as possible. During a specific set of experiments the melting temperature of HNF T_m was highest (114.7°C) when HNF was produced at a small excess of HZ and lowest (111.9°C) when produced at a large excess of HZ. At the same time the VTS values (60°C, 48 h) were 0.67 ml/g and 3.59 ml/g, respectively. Not only from a quality point of view, but also from a yield point of view, it is advantageous to reduce the excess HZ or HZH to the minimum. Constantly measuring the pH during the addition of HZ (HZH) to the NF/DCE mixture and arresting the addition of HZ (HZH) at a more acidic point increased the precipitation yield from 83 to 87%, and VTS data also improved; see batch 4 (reference) and batches 5 and 6 (reduced HZH excess) in Table 2.

d. Filtering and washing of raw HNF on the production day. Normally, HNF is left in the reactor overnight, usually at 15°C, to complete slow reactions. The next day filtering and washing takes place. However, as mentioned before, HNF is incompatible with excess HZ. Therefore, the batches 4, 5, and 6 (see Table 2) have been filtered and washed directly after production, when the temperature is lower. It is clearly seen that this leads to a markedly higher production yield.

e. Recovery of MC/MeOH. Besides high performance, HNF-based propellants have the additional advantage of being environmentally clean. However, this shall not be at the expense of environmental pollution during the production of HNF.

MC and MeOH are used for the washing of HNF. They are the major constituents in the waste stream, which also contains HNF and possibly water, NF, HZ, and DCE. Adding water to the waste stream results in the formation of an inorganic layer containing the HNF, NF, and HZ and a heavier organic layer ($\rho \approx 1300$ kg/m^3). The inorganic layer also contains a certain amount of MeOH as was confirmed by analysis of the recovered inorganic layer. The recovered washing liquid was used in the first washing step of HNF (see Fig. 1). The last washing was performed with virgin washing liquid. No negative effect on the HNF quality could be detected. Altogether, this results in a 35% cost reduction for washing liquids.

2. *Sonocrystallization*

Crystallization under ultrasonic conditions is known to change the crystal properties.[1–4] There are three hypotheses why ultrasound (US) would affect the crystal morphology:

1) It affects the nucleation behavior of the crystallization process.

2) It affects the crystal growth by disturbing the stagnant solution layer adjacent to the solid interface.

3) It breaks the crystals.

There is some supporting experimental evidence for all three mechanisms, but this is insufficient to identify clearly one of these mechanisms as the dominating one. It may well be that all three play a role. All US crystallizations took place at a fixed frequency (20 kHz).

It was investigated whether the crystallization process of HNF is affected by US and, if so, what these effects are. As mentioned before, three crystallization processes are being used. In combination with the C process, excellent improvements in morphology were obtained, first on bench scale and later on pilot scale: L/D (4–8 → 2.6–3.3) and a reduction in the particle size (x_{50}). The results are illustrated in Fig. 4. The following general observations are made for the US C process:

1) With increasing US amplitudes, the particle size distribution increases.

2) With increasing US amplitudes, the aspect ratio and particle size decrease.

3) The thermal stability of HNF crystals (lower gas evolution in VTS) improves.

4) The supersaturation level at which spontaneous nucleation occurs decreases.

In itself, there is no major objection to a somewhat wider particle size distribution because a high solid load in a propellant requires

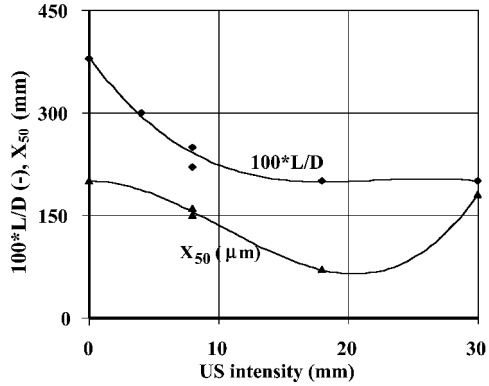

Fig. 4 Effect of US intensity on HNF morphology (bench scale).

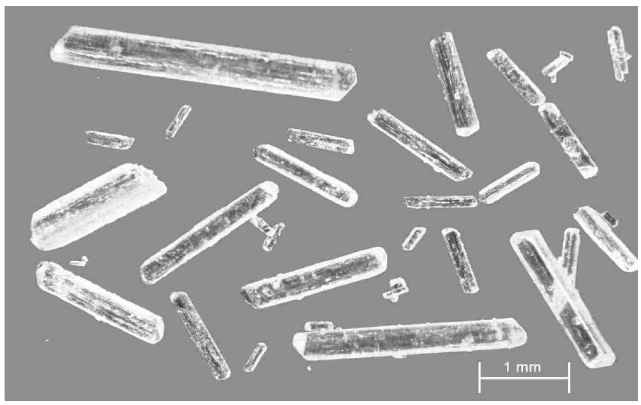

Fig. 5 Cool crystallized HNF.

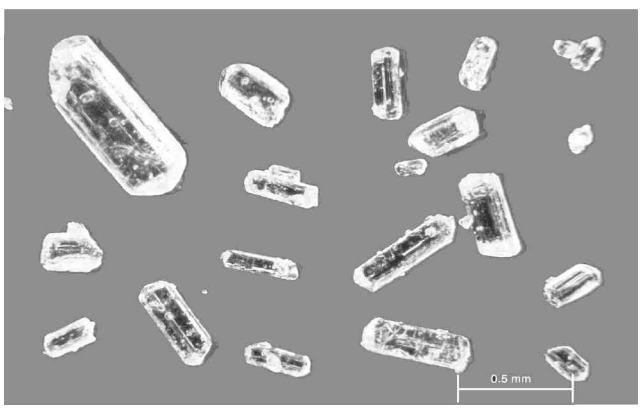

Fig. 6 Cool crystallized HNF under US.

different particle sizes. The particle size has to be controlled, which is possible with US crystallization. The reduction in aspect ratio is a very important improvement in the manufacturing of HNF. This improvement is clearly visible by comparing Fig. 5, which shows HNF manufactured in the pilot plant by the C process, and Fig. 6, which shows HNF manufactured by US-C process. The effect on thermal stability by the US-C process is shown in Figs. 7 and 8. The batches REF-1, REF-2, and REF-3 have been produced without US and the other batches with US. The same level of gas production (5 ml/g) at 60°C is reached 325 (HNF- 2) to 675 (HNF-1 and HNF-3) hours later.

At 80°C the time at which 5 ml/g gas has evolved is 97 h for REF-3, and this increases to 113 h for HNF-2 and HNF-3 and 135 h for HNF-1.

Another important aspect of US crystallization is the strongly increased tap density of the HNF. The improvement in tap density is due to an improved aspect ratio L/D. This is clearly visible in Table 3. Theoretically, the solid load of a propellant is related to the tap density by

Table 3 Effect of US on tap density

Parameter	HNF-1	HNF-2	HNF-3	HNF-C (1995)
US amplitude, μm	20	30	20	0
ρ_{tap}, kg/m^3	1240	1260	1160	1060

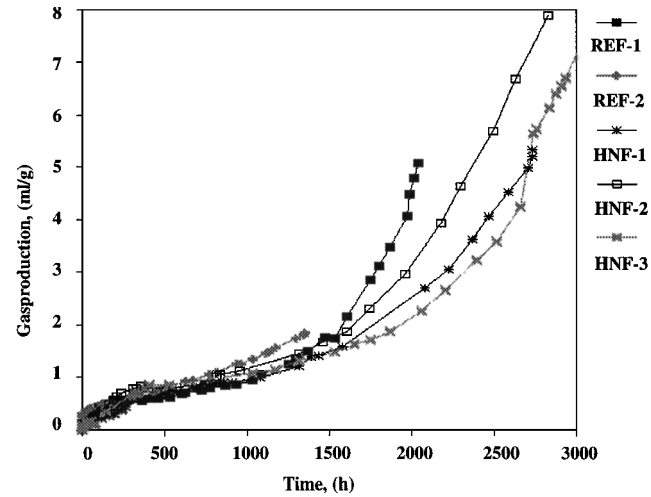

Fig. 7 VTS at 60°C for cool crystallized HNF with (HNF-1, HNF-2, and HNF-3) and without (REF-1 and REF-2) US.

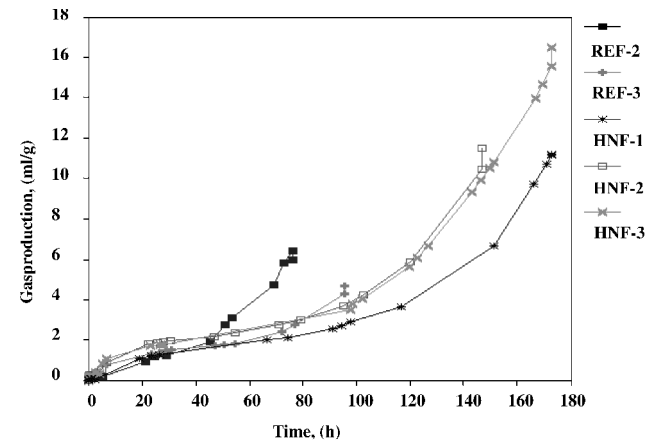

Fig. 8 VTS at 80°C for cool crystallized HNF with (HNF-1, HNF-2, and HNF-3) and without (REF-2 and REF-3) US.

$$S_L = \frac{\rho_{tap} \cdot \rho_{HNF}}{\rho_b \cdot (\rho_{HNF} - \rho_{tap}) + \rho_{HNF} \cdot \rho_{tap}}$$

With $\rho_{HNF} = 1860$ kg/m^3, $\rho_{GAP} = 1300$ kg/m^3, and $\rho_{HTPB} = 900$ kg/m^3, this implies that, with the tap densities of HNF-1 and HNF-2, the solid load for an HTPB/HNF propellant could become 0.75 and 0.76, respectively. With HNF-2 and HTPB, indeed, an experimental propellant[5,6] has been made with a solid load of 0.76.

3. *Cocrystallization*

A special cryogenic crystallization process is not only suitable as an alternative method to crystallize HNF; it also allows easy cocrystallisation of HNF and other ingredients and chemicals.

Typical crystal sizes that were obtained by this method range from <1 to 90 μm, the mean size depending on the applied process parameters. For HNF crystals smaller than 10 μm, $1 \leq L/D \leq 2$. Some properties of cocrystallized HNF are given in Table 4. Cocrystallizing may be done for a number of reasons, including 1) to include a ballistic modifier (e.g., a burning rate modifier) in the oxidizer, or 2) to include a stabilizer in the oxidizer, or 3) to coat the crystals with a protective layer, or 4) to make a premix of HNF and the binder.

Table 4 Some properties of cocrystallised HNF

Property	Cocrystallised HNF			Reference data for HNF
	HNF	HNF+2% stabilizer	HNF+2% coating	
L/D	~1	~1	1–2	1–4 (HNF-C and HNF-S)
D (μm)	~10	~2	~3.5–~7	>40
VTS (60°C, 48 h), ml/g	0.37	0.35	0.75	<1.8
VTS (80°C, 24 h), ml/g	1.8	1.3	3.3	N/A
N_2H_4, wt%	97.6	96.7	96.1	97.2–100.0
H_3O^+, wt%	100.3	101.6	98.7	98.8–100.8
Onset melt, °C	127.5	129	118	129
Onset decomp, °C	128.9	128.9	127	129
Friction Sens., N	20	35	29	14–32
Impact Sens., Nm	2.5	2	3	>2

The inclusion of a burning rate modifier has not been investigated yet, but a number of potential stabilizers has been identified during the development of HNF. Among the ones investigated, the one referred to in Table 4 was very promising. The VTS data themselves indicate a good quality material. The onset decomposition temperature determined by differential scanning calorimetry is identical to standard HNF. Other stabilizers that have been investigated were either not effective or even counterproductive.

Coating of HNF may be done for a number of reasons. The most important one is to shield the HNF from other chemicals that are used in the propellant production process, for example, isocyanates for curing of the binder. It is known that HNF may interact with some isocyanates, hampering the curing process and affecting the aging properties of the propellant. It has been investigated to cocrystallize HNF with a coating material (see Table 4); however, although the VTS data are well within the specifications, the gas evolution has increased compared to pure HNF.

III. HNF Characteristics

A. Stability

Producing HNF using US not only leads to better L/D ratios, but also results in better thermal stability. The HNF with the best stability has also been tested at 90°C. Because data for U.S. HNF[7,8] were available, these are also given in Table 5. In Table 5, three levels of gas evolution, 8, 20, and 23.3 ml/g are given, as well as the time for the various HNF samples to reach this level. The longer the time, the more stable is the product. Note that the U.S. data stem from 1968; Table 5 also demonstrates the progress that has been made over the years.

If it were assumed that the decomposition of HNF is a first-order reaction, the gas production in the VTS would follow from $dG/dt = C = r_T$. The time at different temperatures to produce a well-defined amount of gas may be used to calculate the activation energy from the relation $r_T = A \cdot \exp[-E/(R \cdot T)]$. To determine the activation energy, two good quality types of HNF have been used, HNF-23 and HNF-1. The time to produce 3 ml of gas per gram HNF has been determined at 60, 80, and 90°C, as well as the point where the reaction starts to run away. The results, as well as the determined activation energy, are shown in Table 6. The important aspects are that both types of HNF give the same activation energy (147–157 kJ/mol) and very high values for the correlation coefficients (CC), confirming that the slow (low-temperature) decomposition of HNF essentially is a first-order reaction. One may use these data to estimate the time to generate 3 ml/g gas during normal storage conditions, that is, at 20°C. This is 712 and 610 years, respectively, for HNF 23 and HNF-1, confirming the thermal stability of the material.

Thermogravimetric analysis/mass spectroscopy (TG/MS) measurements during fast decomposition of HNF at 120°C suggested the following species as primary decomposition products: O, NH_3, OH, H_2O, CO, N_2, NO, HCHO, O_2, CO_2, and N_2O, but not NO_2. This may be compared with the decomposition during combustion, which identifies the species NO, O_2, OH, NH, CN, and CH, but also

Table 5 VTS at 90°C for various types of HNF

Gas evolution, ml/g	Time to specified gas evolution (h) for HNF type				
	U.S. Patent 1[7]	U.S. Patent 2[8]	26	1	23
8	14.6	15.3	30.2	34	34.3
20	17.7	20	——	——	46.7
23.3	19	——	——	——	48

Table 6 Experimentally determined activation energy for the slow decomposition of HNF

HNF batch	VTS gas production	Time until gas production is reached, h			E, kJ/mol	CC
		60°C	80°C	90°C		
23	3 ml/g	2675	102	25	157.2	0.9998
	run away	4000	190	50	147.3	0.9999
1	3 ml/g	2225	99	20	157.0	0.9992
	run away	3000	170	35	147.8	0.9980

Table 7 Sensitivity data for HNF

Parameter	Value
BAM fh, J	2–5
BAM ft, N	12–36
R it, figure of impact	33
R rt, figure of friction	1.3–1.5
Critical diameter, mm	<10
Detonation velocity, km/s	8.2–8.5
UN 3(d) response to flame	passed
UN 4(b) 12-m drop test	passed
Electrostatic discharge, mJ	726–4500

NO_2 (see Sec. III.C.1.). Results of earlier decomposition studies using T-jump/FTIR by Williams and Brill[9] for the fast decomposition of HNF in the range of 123–260°C agree with these results for the species, H_2O, CO, NO, and N_2O, and the absence of NO_2, but where Williams and Brill also detected ANF aerosol, $HC(NO_2)_3$, and N_2H_4, these were not observed during the TG/MS measurements at 120°C. On the other hand, Williams and Brill did not report the presence of O, NH_3, OH, N_2, HCHO, O_2, and CO_2. In fact, Williams and Brill state that CO_2 was only detected above 260°C. The differences may be due to different experimental conditions (120°C vs 123–260°C, different heating rates, and different analysis techniques), but it may also be that the improvements in the HNF itself affected the decomposition path.

Although HNF produced nowadays already shows a good thermal stability, this may be further improved by the addition of stabilizers. These may increase the time to a set gas production by ~20% at elevated temperatures. Although the stabilizing mechanism of the most effective stabilizers is not fully understood, it is believed to be caused by scavenging ammonia or the ammonium-ion by forming a complex.

B. Sensitivity

The sensitivities of HNF depend to some extent on the crystallization process (P, E, C, US-C, or S). Four different instruments are being used to determine the friction and impact sensitivity: the Bundes Anstalt für Materialforschung und Prüfung (BAM) fall hammer (BAM fh) and friction tester (BAM ft) and the rotter impact tester (R it) and rotary friction tester (R rt). The main results for HNF are summarized in Table 7.

HNF as an unpackaged material is too friction sensitive at this moment to meet the criteria from the United Nations (UN) Recommendations on the Transport of Dangerous Goods. However, packaged in standard UN boxes, 4.5 kg of HNF passed the UN 4(b) 12-m drop test and, thus, can be transported as 1.1 D material. The sensitivity for electrostatic discharge is very low. Phlegmatizing techniques are under investigation. Phlegmatization of HNF by special gels can increase the friction value well above 80 Nm.

C. Combustion Characteristics, Experimental

1. Decomposition

The decomposition of HNF in hot cell and hot plate experiments has been studied by Louwers[10] and Louwers et al.[11] In the hot cell experiment, HNF is heated in a quartz cell; in the decomposition studies, small amounts of HNF (~50 mg) were dropped into the preheated cell or onto a preheated plate. A UV absorption spectrum is measured, from which an absorption peak at ~280 nm is already found at 110°C, indicating the presence of NO_2 or an aldehyde group. The presence of N_2H_4 or NH_4NO_3 could not be demonstrated. However, one should not conclude that these species are absent in the (early) decomposition products because the N_2H_4 peak may have been shielded off by the absorption peaks of other species in the 230–240 nm region, whereas NH_4NO_3 has a small absorption coefficient. At 130°C, N_2O could also be identified in the 200–220 nm region. Around 160°C, the first HONO is being detected. There are strong indications that HONO itself again decomposes into NO_2: At the bottom of the cell there is a strong HONO signal, at the top of the cell, 45 mm above the HNF, the HONO has virtually disappeared, and there is a strong NO_2 signal. NO was only observed during those experiments where HNF ignited. Finally, it was observed that HNF vapor might be formed during slow heating; this vapor may subsequently condense on colder surfaces. Note that also these results differ somewhat from the experiments by Williams and Brill,[9] who did not report the formation of HONO.

The most likely decomposition mechanism of HNF is a proton transfer, after which N_2H_4 and HONO are released[10] (see Fig. 9). Quantum chemical calculations[10] confirm that the proton transfer has the lowest energy barrier (activation energy 84 kJ/mol). According to these calculations, this is followed by a reaction between the acinitroform and N_2H_4.

2. Neat HNF Samples

For combustion experiments, 6- and 9-mm-diameter samples were pressed at pressures up to 236 MPa; the density of these samples is from 93 to 96% theoretical mean density. The samples have a smooth shiny surface. Under the electron microscope (see Fig. 10), it becomes clear that the individual crystals have, under pressure, more or less formed one single crystal with small voids. Friction sensitivity of pressed HNF has been determined as 16 N and impact sensitivity 10 Nm. The value for friction sensitivity is in the range that has been observed with crystalline HNF. The value for impact sensitivity has increased substantially (decreased sensitivity).

Visual microscopic inspection seems to indicate that the HNF crystals fracture under (high) loads. This discovery led to a way to improve dramatically the HNF morphology[12]: Pressing HNF at 5–6 MPa yields small HNF crystals with $L/D \approx 1$. This method of improving the HNF morphology increases the HNF tap density from 0.65–0.88 g/cm^3 to 1.25 g/cm^3. It was possible to make an HTPB-based HNF propellant[5,6] with a solid load of 78%.

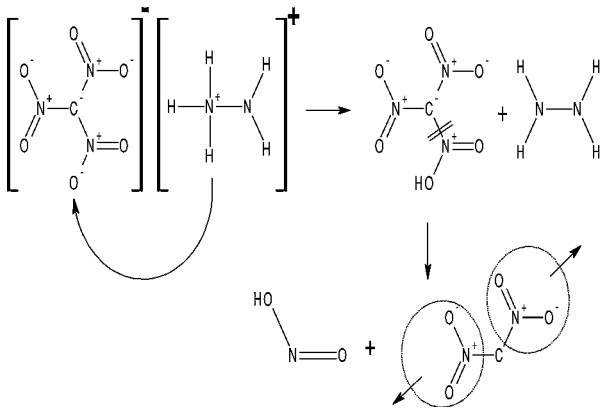

Fig. 9 Proton transfer decomposition of HNF; after the proton transfer N_2H_4 and HONO are released.

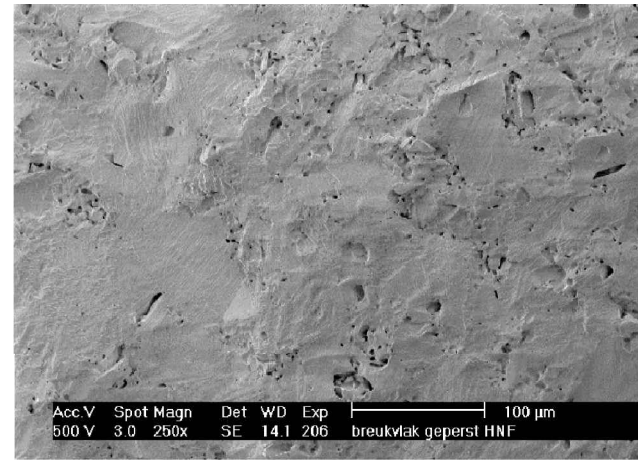

Fig. 10 Fracture of an HNF pellet (electron microscope) showing the fusion of individual crystals.

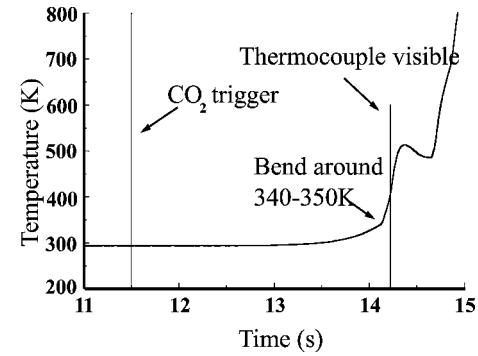

Fig. 11 Temperature history as measured by a microthermocouple embedded in an HNF pellet (0.1 MPa).

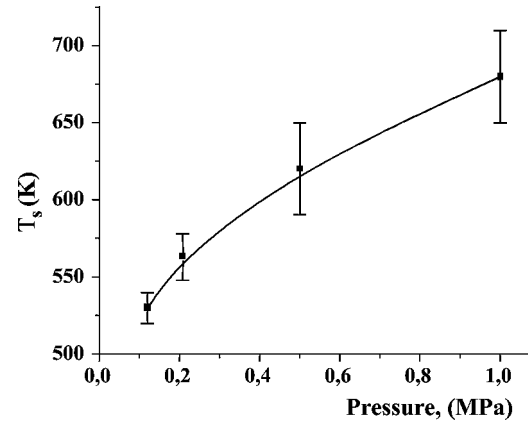

Fig. 12 Measured surface temperature of neat HNF in relation to pressure.

Inserting microthermocouples into neat HNF allowed measuring the HNF temperature profile and surface temperature during burning. Because of thermal stresses, cracks appeared in the pressed HNF pellets during burning, suddenly introducing a thermal resistance in the condensed phase. This effect causes a discontinuity in the thermal profile from around 340 to 350 K (see Fig. 11).

The temperature variation around 14.75 s in Fig. 11 may be explained by the thermocouple loosening itself from the surface. The measured surface temperature of pressed neat HNF is shown in Fig. 12. Note that here at 0.1 MPa a surface temperature of 530 K is measured, whereas McHale and von Elbe[13] measured 553 K for loosely packed HNF at this pressure. Figure 12 clearly indicates a strong variation of surface temperature with pressure in the low-pressure range: from 530 K at 0.1 MPa to 683 K at 1 MPa.

These data agree well with very recently published data by Sinditskii et al.[14] They measured a surface temperature 615 ± 11 K at 0.1 MPa and 698 ± 9 K at 1 MPa. At 2 MPa, Sinditskii et al.[14] measured a surface temperature of 750 ± 10 K.

Within 2 mm above the surface (at ambient pressures), the HNF flame temperature is close to adiabatic. Emission measurements identify NO, O_2, OH, NH, CN, and CH as major species in the flame, whereas absorption measurements indicate that the mole fraction of NO decreases away from the surface. These observations also agree well with those made by Sinditskii et al.[14]: At pressures above 0.1 MPa, the flame temperature measured by Sinditskii et al. is close to the adiabatic flame temperature (from 0.5 to 0.1 mm away from the decomposing HNF surface), whereas in case NO and NO_2 would not have decomposed, the flame temperature would have remained between 1300 and 1600 K.

Pressed neat HNF has a high burning rate with a burning rate exponent $n = 0.95$ for pressures below 2 MPa and $n = 0.85$ at pressures above 2 MPa up to 10 MPa. Sinditskii et al.[14] report $n = 0.92$ and 0.76, respectively.

3. *Samples of HNF and Other Materials*

Pressed samples of 80% HNF and 20% aluminum have an increased burning rate as compared to neat HNF, and the burning rate exponent also increased from 0.95 to 1.02. The high HNF flame temperature close to the surface (0.5 mm above the surface), together with the high OH concentration, leads to a very effective aluminum combustion. Ultrafine aluminum powder (Alex) (20%) yields the highest burn rates with HNF (80%), and the burning rate exponent has been reduced to 0.66.

The addition of 5% burning rate modifier to HNF increases the low-pressure burning rate compared to neat HNF at lower pressures, thereby effectively reducing the burning rate coefficient from 0.95 to 0.81.

IV. Further Developments

In the near future, the focus of HNF development will be on further improving morphology and control of L/D and crystal size during production. Cocrystallization is quite an interesting technology that will be pursued further. It allows coating of the oxidizer crystals and also allows including ballistic modifiers and stabilizers with the HNF. Until recently, a major factor was the friction sensitivity of HNF, which required special measures for transportation and limited the amount of HNF that could be transported. However, in 2000, HNF has been classified as 1.1D for transportation,[15] which allows transport of unrestricted quantities of HNF in wooden boxes.

Implementation of NF production in the existing HNF pilot plant is envisaged to ensure the availability of NF. This will be accompanied by a further overall cost reduction effort in the pilot plant production of HNF. Also, in view of the expected increase in demand, the capacity of the HNF plant may be increased.

V. Conclusions

In a coordinated effort involving a number of research institutes, universities, industries, and agencies, significant improvements and advances in the development of HNF have been achieved. US-C processes led to L/D in the 2–3 range. This is a dramatic improvement compared to the initial crystals, which had L/D values on the order of 15. The cocrystallization method looks very promising for coating of HNF, to reduce friction sensitivity and to include burning rate modifiers. Various detailed experiments have clarified the steady-state combustion processes of HNF. It was possible to model the combustion processes (steady state) with excellent agreement between model and experiment. This has given confidence that the steady-state combustion process is well understood and helps in the propellant formulation for which HNF, after all, is an ingredient.

Acknowledgments

This work was performed under European Space Research and Technology Centre Contracts 11731/95/NL/FG, 12677/97/NL/PA (SC), 13239/98/NL/PA (SC), NIVR Contract NRT 2801 AP, STW Contract DTN66.4108, and private company funding from Fiat Avio and TNO. The authors express their sincere appreciation for the work done by B. d'Andrea and F. Lillo (Fiat Avio, Italy) on the determination of HNF sensitivity, J.M. Bellerby and C.S. Blackman (Cranfield University, U.K.) on the determination and identification of hydrazinium nitroformate (HNF) decomposition mechanisms, M. J. Rodgers and E. J. Marshall (ICI Nobel Enterprises, U.K.) for the work on cocrystallization of HNF, S. Flynn and D. Wagstaff (Royal Ordnance Rocket Motors, U.K.) for determination of HNF sensitivities and investigation of compatibility, E. A. Løkke (NAMMO, Norway) for the characterization of HNF and investigation of compatibility, E. Unneberg (FFI, Norway) for work on the characterization and stabilization of HNF and an investigation of compatibility, and T. Parr and D. Hanson-Parr (Naval Air Weapons Center, United States) for their investigations of the flame structure of HNF and HNF propellants.

References

[1] Hem, S. L., "The Effect of Ultrasonic Vibrations on Crystallisation Processes," *Ultrasonics*, Vol. 5, Oct. 1967, pp. 202–207.

[2] Price, C., "Ultrasound—The Key to Better Crystals for the Pharmaceutical Industry," Pharmaceutical Technology Europe, Publ. 240, an Advanstar publication, Chester, UK, Oct. 1997.

[3] Martin, P., Cains, P., and Price, C., "Sonochemistry," FCW, Dec. 1997, pp. 6–9.

[4] Perkins, J. P., "Power Ultrasonic Equipment for Sonochemistry Research," Sonochemistry Symposium, Annual Chemical Congress, Warwick University, UK, April 1988.

[5] Schöyer, H. F. R., Veltmans, W. H. M., Louwers, J., Korting, P. A. O. G., van der Heijden, A. E. D. M., Keizers, H. L. J., and van den Berg, R. P., "Overview of the Development of HNF-Based Propellants," *Journal of Propulsion and Power*, Vol. 18, No. 1, 2002, pp. 138–145.

[6] Schöyer, H. F. R., Korting, P. A. O. G., Veltmans, W. H. M., Louwers, J., van der Heijden, A. E. D. M., Keizers, H. L. J., and van den Berg, R. P., "Overview of the Development of HNF and HNF-Based Propellants," AIAA Paper 2000-3184, July 2000.

[7] Brown, J. A., "Stabilization of Nitroform Salts," U.S. Patent 3,378,595, April 1968.

[8] Brown, J. A., "Stabilization of Nitroform Salts," U.S. Patent 3,384,675, May 1968.

[9] Williams, G. K., and Brill, T. B., "Thermal Decomposition of Energetic Materials 67. Hydrazinium Nitroformate (HNF) Rates and Pathways Under Combustionlike Conditions," *Combustion and Flame*, Vol. 102, No. 3, 1995, pp. 418–426.

[10] Louwers, J., "Combustion and Decomposition of Hydrazinium Nitroformate (HNF) and HNF Propellants," Ph.D. Dissertation, ISBN 90-9013556-1, Delft Univ. of Technology, Delft, The Netherlands, June 2000.

[11] Louwers, J., Parr, T., and Hanson-Parr, D., "Decomposition and Flame Structure of Hydrazinium Nitroformate," AIAA Paper 99-1091, Jan. 1999.

[12] Louwers, J., and van der Heijden, A. E. D., "Hydrazinium Nitroformate," International Patent Application WO 99/58498, May 1999.

[13] McHale, E. T., and von Elbe, G., "The Deflagration of Solid Propellant Oxidisers," *Combustion Science and Technology*, Vol. 2, 1970, pp. 227–237.

[14] Sinditskii, V. P., Serushkin, V. V., Filatov, S. A., and Egorshev, V. Yu., "Flame Structure of Hydrazinium Nitroformate," *5th International Symposium on Special Topics in Chemical Propulsion (5-ISICP): Combustion of Energetic Materials*, 18–22 June 2000.

[15] United Nations Committee of Experts on the Transportation of Dangerous Goods, ST/SG/AC.10/11 rev. 1, New York, 1990.